Title: Antigen and IL-33 synergistically promote chromatin accessibility at the regulatory regions of pro-inflammatory genes of human skin mast cells

Running title: Antigen and IL-33 promote chromatin accessibility

Authors: Junfeng Gao[1], Yapeng Li[1], Xiaoyu Guan[1], Zahraa Mohammed[2], Gregorio Gomez[3], Yvonne Hui[2], Carole A. Oskeritzian[2], Hua Huang[1, 4]*

Affiliations: [1] Department of Immunology and Genomic Medicine, National Jewish Health, Denver, CO, USA; [2] Department of Pathology, Microbiology and Immunology, University of South Carolina School of Medicine, Columbia, SC, USA; [3] Department of Biomedical Sciences, University of Houston College of Medicine, Houston, TX, USA; [4] Department of Immunology and Microbiology, University of Colorado School of Medicine, Denver, CO, USA.

**Correspondence*:* Dr. Hua Huang, Department of Immunology and Genomic Medicine, National Jewish Health, 1400 Jackson Street, Denver, CO 80206. E-mail address: huangh@njhealth.org

Abstract

Antigenic stimulation through cross-linking the IgE receptor and epithelial cell-derived cytokine IL-33 are potent stimuli of mast cell (MC) activation. However, target genes induced by the combined antigen and IL-33 stimulation have not been investigated in human skin mast cells in a genome-wide manner. Furthermore, epigenetic mechanisms by which IL-33 acts synergically with antigenic stimulation to induce gene transcription have not been investigated. We identified the target genes that responded to the combined antigen and IL-33 stimulation using RNA-seq. These genes can be divided into three groups. Genes in the first group are target genes where antigenic stimulation and IL-33 stimulation achieve high levels of synergy in promoting these gene transcription (high synergy target genes). Genes in the second group are target genes for low levels of synergy mediated by the combined antigen and IL-33 stimulation (low synergy target genes). And genes in the third group are not targeted for the antigen and IL-33 synergy (non-synergy target genes). We found that pro-inflammatory cytokine and chemokine genes were enriched among the high synergy target genes. We demonstrate that the combined antigen and IL-33 stimulation-induced or -increased chromatin accessible areas in the regulatory regions of the high synergy target genes but not of the low synergy target genes. Transcription factor binding motif analysis revealed more binding sites for NF-κB, AP-1, GABPA, and RAP1 in the induced or increased chromatin accessible regions of the high synergy target genes. Our study shines a light on an epigenetic mechanism by which how epithelial cell-derived cytokine IL-33 might cause exacerbation of skin MC-mediated allergic inflammation.

Keywords: Human skin mast cells; IgE receptor cross-linking; IL-33; Chromatin accessibility; Pro-inflammatory genes; Transcription factor NF-κB, AP-1 binding motifs

Introduction

Mast cells (MCs) are long-lived tissue-resident cells with evolutionarily conserved functions in many inflammatory settings, including allergic inflammation and host defense against pathogen infection (Gurish and Austen 2001; Galli et al. 2008). MCs are dispersed throughout the boundaries between the external environment and tissues, such as around blood vessels, in the skin, and at mucosal surfaces. Because of their strategic locations, MCs are among the first exposed to antigenic stimulations and cytokines and chemokines secreted by injured epithelial cells and other inflammatory cells at the site of inflammation.

Epithelial cell-derived cytokines IL-25, IL-33, and TSLP have been reported to activate MCs to amplify inflammation. IL-33 is a member of the IL-1 family (Yagami et al. 2010; Martin and Martin 2016). It is expressed in epithelial cells, dendritic cells, and macrophages in tissues such as the skin, colon, lymph nodes, and lung (Schmitz et al. 2005; Saenz et al. 2008). IL-33 protein is released from injured epithelial cells in infections and inflammation as IL-33 stored in the nucleus of destroyed epithelial cells is set free (Saluja et al. 2015; Martin and Martin 2016). In fact, MCs express high levels of IL-33 (IL1RL1) receptor (Lohning et al. 1998; Moritz et al. 1998; Allakhverdi et al. 2007b). IL-33 activates MAP kinases and induces NF-κB phosphorylation (Schmitz et al. 2005). IL-33 promotes the differentiation of MC progenitor cells into mature MCs that produce Th2 cytokines IL-5 and IL-13 (Allakhverdi et al. 2007b). It directly activates MCs to produce pro-inflammatory cytokines and chemokines, including IL-6, IL-10, TNF, GM-CSF, CXCL8, and CCL1 (Bawazeer and Theoharides 2019; Franke et al. 2021). It synergizes with TSLP to promote MC differentiation and activation (Saluja et al. 2016).

IL-33 also synergized with IgE receptor activation of primary human MCs to promote CXCL8, IL-4, and IL-13 production (Silver et al. 2010). IL-33 plays an important role in promoting IgE-mediated allergic inflammation (Kato et al. 2021). IL-4, IL-5, and IL-13 were increased in ovalbumin (OVA)-sensitized mice treated with IL-33, compared with mice treated with IL-33 alone or OVA alone (Sjoberg et al. 2017). Activated by antigenic stimulation, NFAT acts synergistically with NF-κB, which is activated by IL-33, to promote luciferase gene transcription under the control of multiple copies of NFAT/AP1 and NF-κB binding sites (Andrade et al. 2011). TSLP is a potent MC activator (Allakhverdi et al. 2007a; Saluja et al. 2016). It induces pro-inflammatory cytokines and chemokines IL-5, IL-33, IL-6, GM-CSF, CXCL8, and CCL1 in the presence of IL-1 and TNF in human MCs (Allakhverdi et al. 2007a). TSLP-deficient mice have reduced numbers of MCs, showing attenuated mast cell-mediated allergic reactions (Han et al. 2014). Thus, a complex network of gene-gene and cell-cell interactions initiated by epithelial cells and MCs can exacerbate inflammation.

Antigenic stimulation through cross-linking the IgE receptor (IgECL) is a strong stimulus for promoting *de novo* gene transcription. IgECL upregulated expression of 1089 genes and downregulated 280 genes in mouse MCs (Li et al. 2021). The upregulated genes were significantly enriched in gene sets encoding signaling molecules, cell surface molecules, cytokines and chemokines, transcription factors, proteases, and other enzymes. In comparison, the repressed genes were significantly enriched in gene sets involved in cell proliferation, signal transduction, and apoptosis (Akula et al. 2020; Li et al. 2021). In human MCs, antigenic stimulation upregulated hundreds to thousands of genes while downregulating tens to hundreds of genes (Motakis et al. 2014; Cildir et al. 2019). The stimulation with IL-33 induced 823 genes

in mouse MCs, including *Ccl1*, *Egr2*, and *Il1b*. IL-33-upregulated genes included genes regulated by NF-κB and STAT3 in response to TNF, IL-6, and IFN-γ (Chhiba et al. 2017). Although it has been reported that IL-33 acts synergistically with antigenic stimulation to promote some cytokine and chemokine gene transcription, other target genes synergistically upregulated by the combined antigen and IL-33 stimulation have not been investigated using a genome-wide approach. Furthermore, epigenetic mechanisms by which IL-33 acts synergically with antigenic stimulation to induce gene transcription have not been investigated.

In this study, we identified the target genes that responded to the combined antigen and IL-33 stimulation using RNA sequencing (RNA-seq). We found that many genes that responded to the combined antigen and IL-33 stimulation have not been reported to be target genes before, including genes that encode signal molecules, transcription factors, molecules involved in cell survival and cell death, and receptor and receptor binding molecules. We demonstrate that the combined antigen and IL-33 stimulations induced or increased chromatin accessible areas in the regulatory regions of the high synergy target genes but not in the low synergy target genes. Transcription factor binding motif analysis revealed more binding sites for NF-κB, AP-1, GABPA, and RAP1 in the induced or increased chromatin accessible regions of the high synergy target genes. Our study shines a light on an epigenetic mechanism by which IL-33 might cause exacerbation of skin MC-mediated allergic inflammation.

Results

The combined antigen and IL-33 stimulation promote expression of two clusters of genes

To determine whether epithelial cell-derived cytokines IL-33, IL-25, TSLP, and antigenic stimulation mediated by IgE receptor cross-linking (IgECL) can synergistically induce gene expression in human skin mast cells (HSMCs), we performed RNA-seq analysis on HSMCs that were not stimulated or stimulated with IgECL, IL-25, TSLP or IL-33 alone or in combinations. Although a small number of early response genes can respond to cytokine stimulation, most genes need longer time of priming to be able to respond. We thus treated HSMCs overnight. Antigenic stimulation, on the other hand, can induce rapid gene responses. And we treated HSMCs with antigen via IgECL for two hours. IgECL alone upregulated 501 genes with increased expression greater than 2-fold and 37 genes with increased expression greater than 10-fold (**Figure E1, *A* and Table E1, sheet 1**). We found that IL-33 stimulation upregulated 259 genes that were expressed 2-fold greater and 22 genes with increased expression greater than 10-fold (**Figure E1, *B* and Table E1, sheet 2**). Whereas IL-25 only upregulated nine genes greater than 2-fold with none of the genes increased expression greater than 10-fold (**Figure E1, *C* and Table E1, sheet 3**). TSLP upregulated 17 genes greater than 2-fold with one gene increased expression greater than 10-fold (**Figure E1, *D* and Table E1, sheet 4**). These results indicate that the combined antigen and IL-33 stimulation are potent stimuli in upregulating genes in primary HSMCs.

To determine whether any of the combinatorial stimulations upregulate HSMC genes, we used the K mean clustering method to group genes into clusters with similar expressions. We first determined the optimal K numbers of six using Elbow Plot (**Figure E2**). Heatmap K means clustering analysis revealed that the combined IL-33 and IgECL stimulations upregulated expression of two major clusters of genes (cluster four and cluster six) relative to IgECL or IL-33 single stimulation (**Figure 1**). There were 902 genes in cluster four and 641 genes in cluster six (**Table E2**). IL-25 and TSLP, when added with IgECL, also promoted expression of genes in cluster four. However, they were weaker promoters. IL-25 and IgECL upregulated 50 genes compared with IgECL alone (**Figure E3, *A* and Table E3, sheet 1**). TSLP and IgECL upregulated 27 genes compared with IgECL alone (**Figure E3, *B* and Table E3, sheet 2**). Addition of IL-25 and TSLP to the IgECL and IL-33 combination did not significantly alter MC gene expression profiles compared with the IgECL and IL-33 combination (**Figure E3, *C* and Table E3, sheet3**). These results demonstrated that epithelial cell-derived cytokines IL-33 together with IgECL to promote expressions of cluster four and six human skin MC genes.

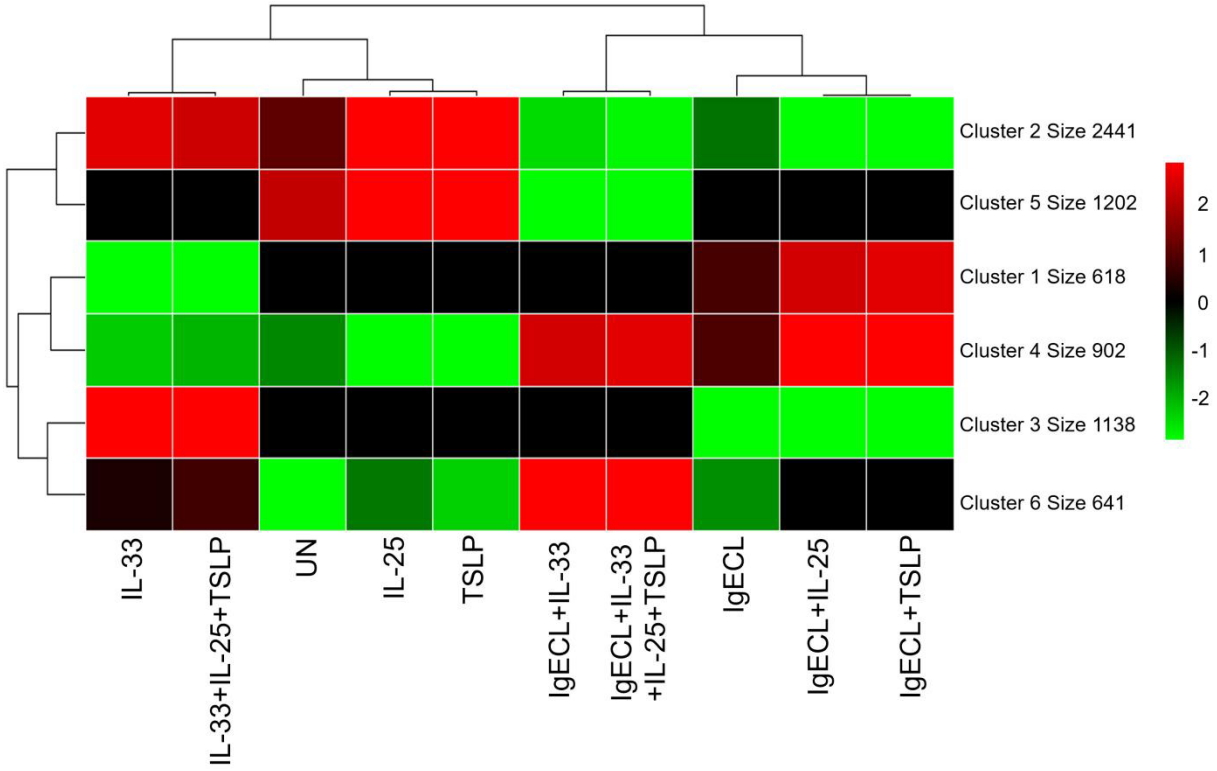

Figure 1. IL-33 acts synergically with IgE receptor cross-linking to promote gene transcription in clusters four and six. Human skin mast cells were not stimulated (UN) or stimulated with IgE receptor cross-linking (IgECL), IL-33, IL-25, or TSLP alone or in combinations as indicated. K-means clustering analysis was performed using R package pheatmap. The cluster size numbers indicate the number of genes that are grouped in the cluster. RNA-seq data were generated from two biological samples.

The combined antigen and IL-33 stimulation synergistically induce pro-inflammatory gene transcription

We performed gene ontology (GO) analysis on genes in clusters four and six to determine which types of genes were enriched among genes that were promoted by the combined antigen and IL-33 stimulation. We found that genes encoding for cytokines (Cluster four, $p=1.0\times10^{-5}$; cluster six, $p=2.5\times10^{-5}$, **Figure 2, *A***), receptors and receptor binding (Cluster four, $p=7.9\times10^{-2}$; cluster

six, $p=3.6\times10^{-2}$, **Figure 2, *A***), signaling molecules (Cluster four, $p=9.7\times10^{-6}$; cluster six, $p=7.3\times10^{-3}$, **Figure 2, *A***), transcription factors (Cluster four, $p=1.8\times10^{-2}$; cluster six, $p=2.6\times10^{-3}$, **Figure 2, *A***), NF-κB signaling pathway (Cluster four: $p=6.5\times10^{-2}$, cluster six: $p=4.2\times10^{-2}$, **Figure 2, *A***), chemokines (Cluster four: $p=1.1\times10^{-5}$; cluster six, $p=9.7\times10^{-2}$, **Figure 2, *A***), and molecules involved in cell death (Cluster four, $p=2.6\times10^{-2}$; cluster six: $p=1.7\times10^{-2}$, **Figure 2, *A***) were significantly enriched in both clusters (**Figure 2, *A***).

A

Go analysis

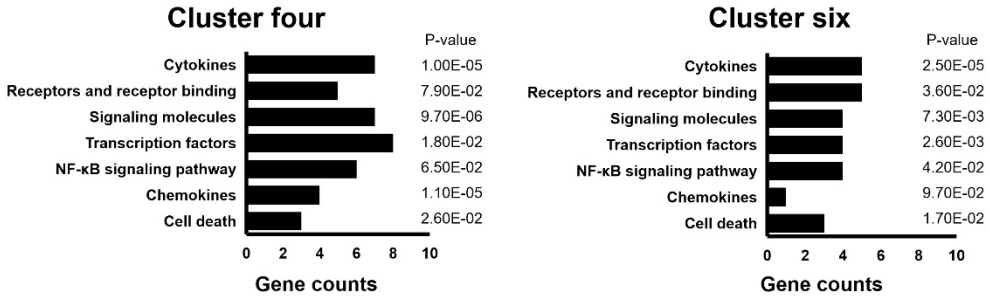

B

Representative genes

Cluster four

Cytokines and chemokines

Gene	UN	IL33	IgECL	E+33	Log2 ratio E+33/E	Log2 ratio E+33/33
CXCL8	15.6	6.0	185.1	5533.2	4.9	9.8
CXCL3	0.4	0.3	2.8	155.9	5.8	9.3
TNFSF4	5.4	2.2	12.7	48.4	1.9	4.5
IL33	0.9	0.5	1.6	10.9	2.7	4.4
IL6	10.9	17.7	54.7	229.0	2.1	3.7
CCL20	0.0	0.9	2.6	12.2	2.2	3.8
IL23A	0.2	0.3	0.6	10.4	4.1	5.2
CCL1	36.9	106.0	199.6	1173.5	2.6	3.5
CXCL2	0.3	1.0	1.7	144.0	6.4	7.2
IL13	1.3	4.4	6.6	21.7	1.7	2.3
VEGFA	51.6	66.6	94.4	196.9	1.1	1.6

Receptors and receptor binding

Gene	UN	IL33	IgECL	E+33	E+33/E	E+33/33
CD200	0.1	0.3	8.9	19.0	1.1	6.0
DUSP1	9.6	6.5	19.8	46.7	1.2	2.9
CD274	17.5	13.0	36.5	89.9	1.3	2.8
LRP12	9.8	10.1	13.5	31.5	1.2	1.6
HEG1	5.6	7.1	7.6	26.2	1.8	1.9

Signaling molecules

Gene	UN	IL33	IgECL	E+33	E+33/E	E+33/33
RGS2	126.8	63.6	288.6	596.1	1.0	3.2
RGS16	3.1	1.9	7.2	25.8	1.8	3.7
GADD45A	12.4	17.8	54.1	147.1	1.4	3.1
VCAN	2.9	2.6	4.0	10.3	1.4	2.0
LAPTM4B	12.2	6.5	8.5	17.4	1.0	1.4

Transcription factors

Gene	UN	IL33	IgECL	E+33	E+33/E	E+33/33
EGR4	0.4	0.1	4.1	14.3	1.8	7.3
CREB5	1.3	0.4	5.9	19.8	1.7	5.8
MLF1	2.0	1.7	6.6	18.6	1.5	3.4
ZFP36L2	82.4	43.3	154.0	461.2	1.6	3.4
RFX2	2.6	8.0	21.1	52.3	1.3	2.7
CEBPD	4.1	5.9	13.0	32.7	1.3	2.5

NF-κB signaling pathway

Gene	UN	IL33	IgECL	E+33	E+33/E	E+33/33
NFKB1	20.1	38.6	40.1	112.2	1.5	1.5
REL	10.1	8.7	22.7	67.4	1.6	2.9
TNFRSF21	5.5	4.0	6.7	20.3	1.6	2.4
MAP3K8	12.9	19.3	67.0	146.1	1.1	2.9
GBP2	38.4	27.2	82.5	179.3	1.1	2.7
RIPK2	17.8	22.9	27.7	92.0	1.7	2.0

Cell death

Gene	UN	IL33	IgECL	E+33	E+33/E	E+33/33
BCL2A1	5.6	4.7	41.9	94.0	1.2	4.3
BCL6	6.0	5.7	7.2	17.8	1.3	1.7
ACKR3	2.3	8.8	9.5	29.1	1.6	1.7

Cluster six

Cytokines and chemokines

Gene	UN	IL33	IgECL	E+33	Log2 ratio E+33/E	Log2 ratio E+33/33
IL1B	0.3	53.8	0.6	367.7	9.2	2.8
IL5	0.2	6.5	0.4	35.9	6.6	2.5
VEGFC	1.8	4.4	2.1	10.2	2.3	1.2
CSF3	0.2	1.2	0.9	17.4	4.3	3.8
CXCL1	0.6	1.2	1.1	17.4	3.9	3.9
IL1A	1.3	3.9	3.9	29.6	2.9	2.9

Receptors and receptor binding

Gene	UN	IL33	IgECL	E+33	E+33/E	E+33/33
IL7R	0.6	21.8	1.5	48.3	5	1.1
FCGR2A	10	27.9	7.3	57.5	3	1
TNFRSF9	0.4	9.9	2.9	20.9	2.8	1.1
MFSD2A	0.8	7.4	3.2	33.3	3.4	2.2
HLA-E	343.4	460.3	434.2	991.9	1.2	1.1

Signaling molecules

Gene	UN	IL33	IgECL	E+33	E+33/E	E+33/33
MTSS1	14.6	42	28.8	96.3	1.7	1.2
ITK	8.3	8.2	7	23.9	1.8	1.5
FSTL1	12.2	10.6	10.1	21.7	1.1	1

Transcription factors

Gene	UN	IL33	IgECL	E+33	E+33/E	E+33/33
SKIL	5.6	14.3	5.3	32.5	2.6	1.2
TWIST2	9.6	16.8	14.9	36	1.3	1.1
YBX3	14.6	20.5	18.3	41.6	1.2	1
TWIST1	11.3	23.9	21.5	49.5	1.2	1

NF-κB signaling pathway

Gene	UN	IL33	IgECL	E+33	E+33/E	E+33/33
TNFAIP3	3.7	28.9	11.6	65.1	2.5	1.2
NFKBIA	173.3	283.5	173	575.5	1.7	1
NFKBIZ	48.4	76.7	68.2	201	1.6	1.4
TNFAIP2	4.1	8.3	6.7	23	1.8	1.5

Cell death

Gene	UN	IL33	IgECL	E+33	E+33/E	E+33/33
NINJ1	21	59.5	33.4	141	2.1	1.2
G0S2	14.2	42.4	39.9	95.4	1.3	1.2
TNFAIP8	48	43.5	30.3	93.3	1.6	1.1

Figure 2. Genes upregulated by the synergistic stimulation of IL-33 and IgE receptor cross-linking are enriched in genes encoding pro-inflammatory cytokines and chemokines. A. Gene ontology (GO) enrichment analysis of the upregulated genes in clusters four and six. *P*-values were calculated by a one-side Fisher's exact test with the adjustment of Benjamini-Hochberg method. **B.** Heatmap representation of top ranked genes in each gene family in clusters four and six. The numbers indicate RNA reads (FPKM). Log2 E+33/E, log2 ratio of reads of IgECL+IL-33 stimulated to reads of IgECL stimulated; log2 E+33/33, log2 ratio of reads of IgECL+IL-33 stimulated to reads of IL-33 stimulated. Data represent the average reads generated from two biological samples.

The top ranked representative genes in clusters four and six are listed in **Figure 2B**. Genes encoding cytokines and chemokines family in cluster four were most significantly enriched. They include *CXCL8*, *CXCL3*, *TNFSF4*, *IL33*, *IL6*, *CCL20*, *IL23A*, *CCL1*, *CXCL2*, *IL13* and *VEGFA* (**Figure 2, *B***). Genes enriched in the cytokines and chemokines gene family in cluster six include *IL1B*, *IL5*, *VEGFC*, *CSF3*, *CXCL1* and *IL1A.* While *CXCL8*, *IL5*, *IL13*, and *IL6* have been reported to be upregulated synergistically by the combined IL-33 and antigen stimulation (Andrade et al. 2011), *TNFSF4*, a member of TNF family, *CXCL3*, *IL33*, *CCL20*, *IL23A*, *CCL1*, *CXCL2*, *CXCL1*, *VEGFC*, *CSF3*, *IL1A* and *VEGFA*, a growth factor for vascular endothelial cells (Dvorak et al. 1979; Brown et al. 1997), have not been reported as target genes of the combined IL-33 and antigen stimulation in HSMCs.

Genes encoding signaling molecules in cluster four were also highly enriched (**Figure 2, *A***). These genes include *RGS2*, which potently interferes with signaling through receptors that couple to GQα (Kehrl and Sinnarajah 2002), *RGS16*, which inhibits signal transduction through the Gα13-RHO (Johnson et al. 2003). *MTSS1* and *ITK* were enriched in cluster six (**Figure 2, *B***). These genes were not reported previously as target genes for the synergistic stimulation of IL-33 and antigen. We also found that genes encoding receptor and receptor binding molecules were

significantly enriched in clusters four and six (**Figure 2, *B***). These genes included *IL7R*, a receptor for IL-7 and TSLP (Noguchi et al. 1993; Pandey et al. 2000; Park et al. 2000), *FCGR2A*, which encodes a cell surface receptor belong a family of immunoglobulin Fc receptor, *CD274*, encoding PD-L1, a ligand that binds to the receptor PD1 commonly found on T-cells to block T-cell activation (Keir et al. 2006; Noman et al. 2014) (**Figure 2, *B***).

Many genes encoding molecules involved in cell survival and cell death were identified in clusters four and six (**Figure 2, *B***). *BCL2A1* is a highly regulated NF-κB target gene that exerts important pro-survival functions (Vogler 2012). BCL6 acts to prevent apoptotic cell death in differentiating myocytes (Kumagai et al. 1999). *ACKR3*, which encodes a receptor for CXCL12 and CXCL11 (Burns et al. 2006), has been reported to inhibit apoptosis (Hattermann et al. 2010). TNF Alpha Induced Protein 8 (TNFAIP8) can increase cell survival and decrease apoptosis in hepatocellular carcinoma cells (Niture et al. 2020). On the other hand, we also found that IL-33 and IgECL stimulation upregulated genes involved in apoptosis, including *G0S2*, which promotes apoptosis by binding to BCL2. *NINJ1*, which encodes NINJURIN-1 (Araki and Milbrandt 1996), has been shown to promote apoptosis in macrophages during early ocular development (Lee et al. 2009).

Genes encoding transcription factors were found to be significantly enriched in clusters four and six (**Figure 2, *A***). EGR4, activated by NFAT in response to antigenic stimulation and regulates pro-inflammatory cytokine gene expression (Decker et al. 2003), CEBPD results in increased *IL6* gene transcription (Hungness et al. 2002). Transcription factors *CREB5*, *MLF1*, *ZFP36L2* and *RFX2* were enriched in cluster four, while transcription factors *SKIL*, *TWIST2*,

YBX3 and *TWIST1* were enriched in cluster six (**Figure 2, *B***). Genes encoding NF-κB signaling pathway were also highly enriched in both clusters four and six (**Figure 2, *A***). These genes included *NFKB1*, encoding p50 subunit of NF-κB transcription factor complex that can lead to amplified transcription outputs for many of the NF-κB target genes, such as *IL1B*, *IL6*, *CXCL8*, *TNF*, *MCP1*, *CXCL1* (Liu et al. 2017). *REL*, *TNFRSF21*, *MAP3K8*, *GBP2* and *RIPK2* were enriched in cluster four, while *TNFAIP3*, *NFKBIA*, *NFKBIZ* and *TNFAIP2* were enriched in cluster six (**Figure 2, *B***).

We observed that some genes were upregulated by the combined antigen and IL-33 stimulation more than the others. To assess the responsiveness of genes in clusters four and six to the combined antigen and IL-33 stimulation, we calculated the log2 ratios of RNA-seq reads derived from IgECL and IL-33 treatment over reads derived from IgECL or IL-33 treatment alone. The average log2 ratio of IgECL+IL-33/IgECL for genes in cluster four is 1.8 and the average log2 ratio of IgECL+IL-33/IgECL for genes in cluster six is 2.7. The average log2 ratio of IgECL +IL-33/IL-33 in cluster four is 3.4 and the average log2 ratio of IgECL+IL-33/IL-33 in cluster six is 1.6 (**Figure 2, *B*, Table E4**). The log2 ratio analysis indicated that genes in cluster four tended to have higher ratios of IgECL+IL-33 over IL-33 because these genes had lower responsiveness for IL-33 stimulation alone, whereas genes in cluster six tended to have higher ratios of IgECL+IL-33 over IgECL because the cluster six genes had lower responsiveness for IgECL alone (**Figure 2, *B***).

Based on the log2 ratio calculations, genes whose transcripts were promoted by the combined antigen and IL-33 stimulation can be divided into two categories: Genes responsive to the synergistical action of the combined antigen and IL-33 stimulation and genes that did not

respond to the synergistical action of the combined antigen and IL-33 stimulation. In the first group where genes were the targets for the antigen and IL-13 synergy, we further divided the genes into genes highly responsive and genes moderately responsive. We defined genes highly responsive to the combined IgECL+IL-33 stimulation as those genes having both log2 ratios of IgECL+IL-33/IL-33 and log2 ratios of IgECL+IL-33/IgECL greater than 1.5 (2.8-fold increase). We defined genes moderately responsive to the combined IgECL+IL-33 stimulation as those genes having both log2 ratios of IgECL+IL-33/IL-33 and log2 ratios of IgECL+IL-33/IgECL greater than 1, but less than 1.5. According to these criteria, 19 genes were considered as highly responsive genes (referred to as high synergy target genes) and 9 genes as moderately responsive genes (referred to as low synergy target genes). High synergy target genes include *IL1B*, *MFSD2A*, *XIRP1*, *TNFSF4*, *CXCL2*, *RIPK2*, *ZFP36L2*, *PALLD*, *CXCL3*, *NAMPT*, *IL6*, *IL5*, *CCL1*, *SERPINE1*, *SLCO4A1*, *CXCL8*, *REL*, *C11orf96* and *MT2P1*. Low synergy target genes include *DENND5A*, *LAPTM4B*, *G0S2*, *YBX3*, *RPL36AP26*, *FSTL1*, *HLA-E*, *TWIST1*, and *TWIST2* (**Table E5**). We noted that proinflammatory cytokine and chemokine genes were significantly enriched among the 19 high synergy target genes. We found that the majority of genes in clusters four and six were non-synergy target genes, they did not respond to the synergistic action of the combined IgECL and IL-33 stimulation as these genes had both log2 ratios of IgECL+IL-33/IL-33 and log2 ratios of IgECL+IL-33/IgECL less than 1 (less than 2-fold increase).

We performed a qPCR analysis on several high synergy target genes *CCL1*, *IL1B*, *NAMPT* and *CXCL8* genes in HSMCs derived from four deidentified individuals. We showed that *CCL1* mRNA was synergistically upregulated by IgECL and IL-33 (Log2 ratio=3.2 (8.9-fold increase)

relative to IL-33 stimulation alone; Log2 ratio=1.9 (3.7-fold increase) relative to IgECL alone) (**Figure 3**). We verified that IgECL alone did not noticeably promote *IL1B* gene transcription, while IL-33 alone moderately promoted *IL1B* gene transcription. But the combined IgECL and IL-33 stimulation led to dramatic synergistical increase in *IL1B* gene transcription (Log2 ratio=2.0 (4.1-fold increase) relative to IL-33 stimulation alone; Log2 ratio=8.0 (248-fold increase) relative to IgECL alone) (**Figure 3**). Synergistical increases in gene transcription promoted by the combined IgECL and IL-33 stimulation were also confirmed for the *NAMPT* gene (Log2 ratio=3.4 (10.3-fold increase) relative to IL-33; Log2 ratio=2.1 (4.2-fold increase) relative to IgECL) and *CXCL8* gene (Log2 ratio=4.2 (17.9-fold increase) relative to IL-33; Log2 ratio=2.2 (4.6-fold increase) relative to IgECL) (**Figure 3**). We demonstrated that the log 2 ratios of IgECL+IL-33 to IgECL alone or IgECL+IL-33 to IL-33 were remarkably similar between results obtained from RNA-seq analysis and qPCR analysis.

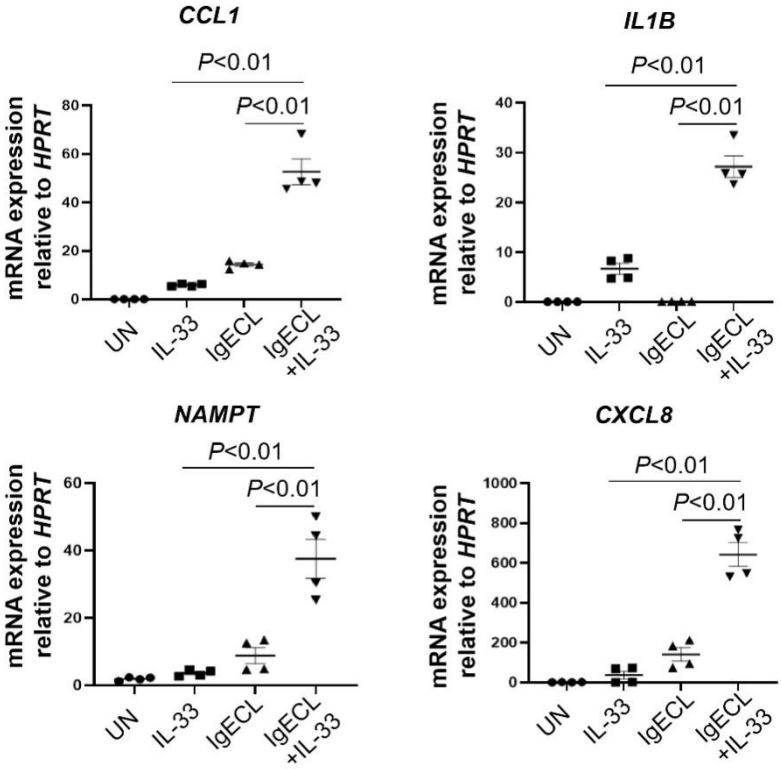

Figure 3. Validation of gene expression promoted by the combined IgECL and IL-33 stimulation. HSMCs were not stimulated (UN) or stimulated with IgE receptor cross-linking (IgECL), IL-33, or in combination of IgECL and IL-33. qPCR analysis of the mRNA expression of activation-induced genes identified by RNA-seq. *P* values were calculated using one-tailed student's *t* test. Data represents mean ± SEM of four biological samples.

The combined antigen and IL-33 stimulation synergistically increase chromatin accessibility in the high synergy target genes, but not the low synergy target genes

Enhancers integrate signal inputs and convert them into transcriptional outputs (Spitz and Furlong 2012). Thus, it is likely that the combined IgECL and IL-33 stimulation activate signal-dependent transcription factors that, in turn, bind to enhancers to increase chromatin accessibility at the enhancers of genes responding to the combined antigen and IL-33 stimulation. To investigate how the combined IgECL and IL-33 stimulation synergistically affect chromatin accessibility, we performed Omni-ATAC-seq analysis on HSMCs that were treated with IgECL or IL-33 alone or with both IgECL and IL-33. We used differential bind analysis (Diffbind) to compare ATAC-seq broad and narrow peaks from the IgECL and IL-33 stimulation-treated HSMCs with those from either IL-33- or IgECL-treated HSMCs. We assigned ATAC-seq peaks located within 100 kb upstream or downstream from TSS to a gene using Binding and Expression Target Analysis (BETA). Tens of thousands of narrow peaks (21,451), which were significantly enriched peaks compared to pooled and normalized background, increased significantly in the IgECL and IL-33-treated HSMCs compared to IL-33. Fewer narrow peaks (521) were found to be significantly elevated when compared with IgECL (**Table E6**).

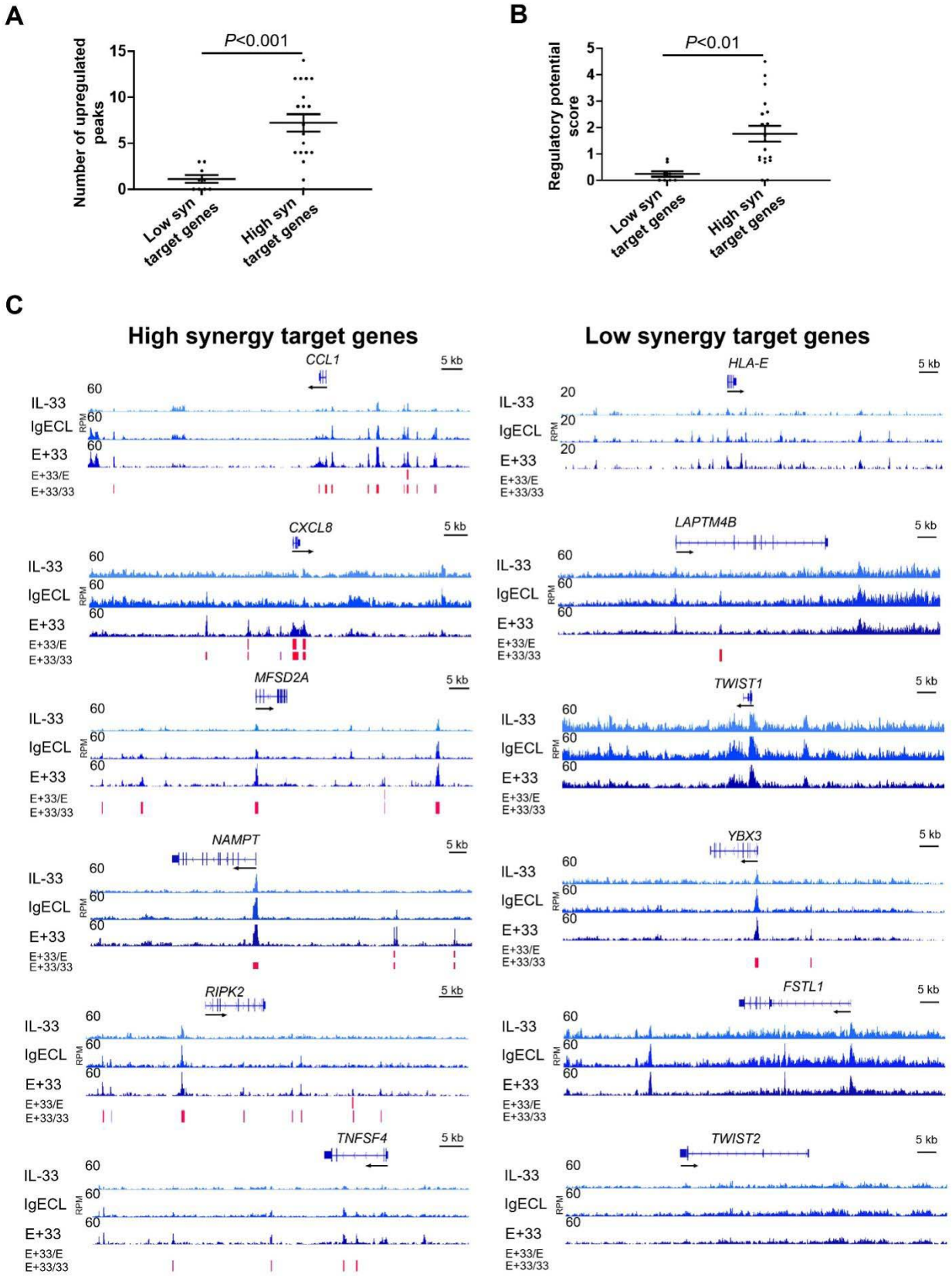
A
P<0.001
Number of upregulated peaks
15
10
5
0
Low syn target genes
High syn target genes
B
P<0.01
Regulatory potential score
5
4
3
2
1
0
Low syn target genes
High syn target genes
C
High synergy target genes
Low synergy target genes
CCL1
HLA-E
CXCL8
LAPTM4B
MFSD2A
TWIST1
NAMPT
YBX3
RIPK2
FSTL1
TNFSF4
TWIST2
5 kb
IL-33
IgECL
E+33
E+33/E
E+33/33
RPM
60
20

281

Figure 4. IL-33 and IgE receptor cross-linking synergistically increase chromatin accessibility in the high synergy genes. A. The numbers of upregulated ATAC-seq narrow peaks in the combined IgECL and IL-33 stimulation relative to IgECL or IL-33 stimulation were subtracted using Diffbind analysis. **B.** Regulatory potential scores were calculated by BETA. *P* values were calculated using the one-tailed Student's *t* test. **C.** Representative tracks of the ATAC-seq broad peaks and narrow peaks (marked in red). RPM, reads per million nucleotides mapped; Low synergy target genes (Low syn target genes); High synergy target genes (High syn target genes). Data shown in A represent two biological samples. The IGV tracks are generated from one biological sample, representing two biological replicates with similar patterns.

To determine the mechanism by which antigen stimulation acts synergistically with IL-33 to promote pro-inflammatory gene transcription, we analyzed the differences in the number of upregulated narrow peaks in the nine low synergy target genes and 19 high synergy target genes. We counted the numbers of significantly increased narrow peaks located in the low synergy target genes or high synergy target genes and found that 6.5-fold greater in the high synergy target genes than those in the low synergy target genes (**Figure 4, *A***). Regulatory potential scores are designed to measure the number of accessible regions as well as the locations of the accessible regions relative to the transcription start site (TSS) (Wang et al. 2013). We found that the high synergy target genes scored higher in the regulatory scores than the low synergy target genes (7.4-fold, **Figure 4, *B***). Representative ATAC broad and narrow peaks (marked in red) in the low and high synergy target genes are shown in **Figure 4C**.

A

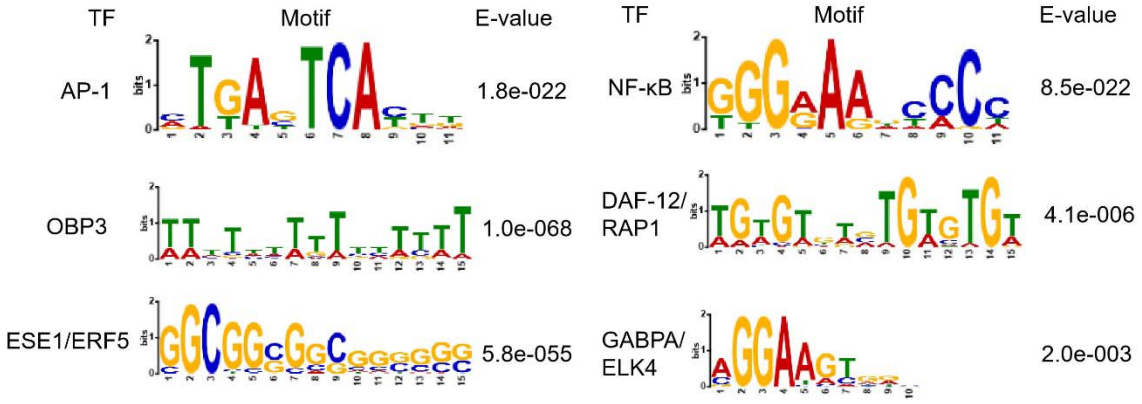
TF
Motif
E-value
AP-1
1.8e-022
OBP3
1.0e-068
ESE1/ERF5
5.8e-055
TF
Motif
E-value
NF-κB
8.5e-022
DAF-12/
RAP1
4.1e-006
GABPA/
ELK4
2.0e-003

B

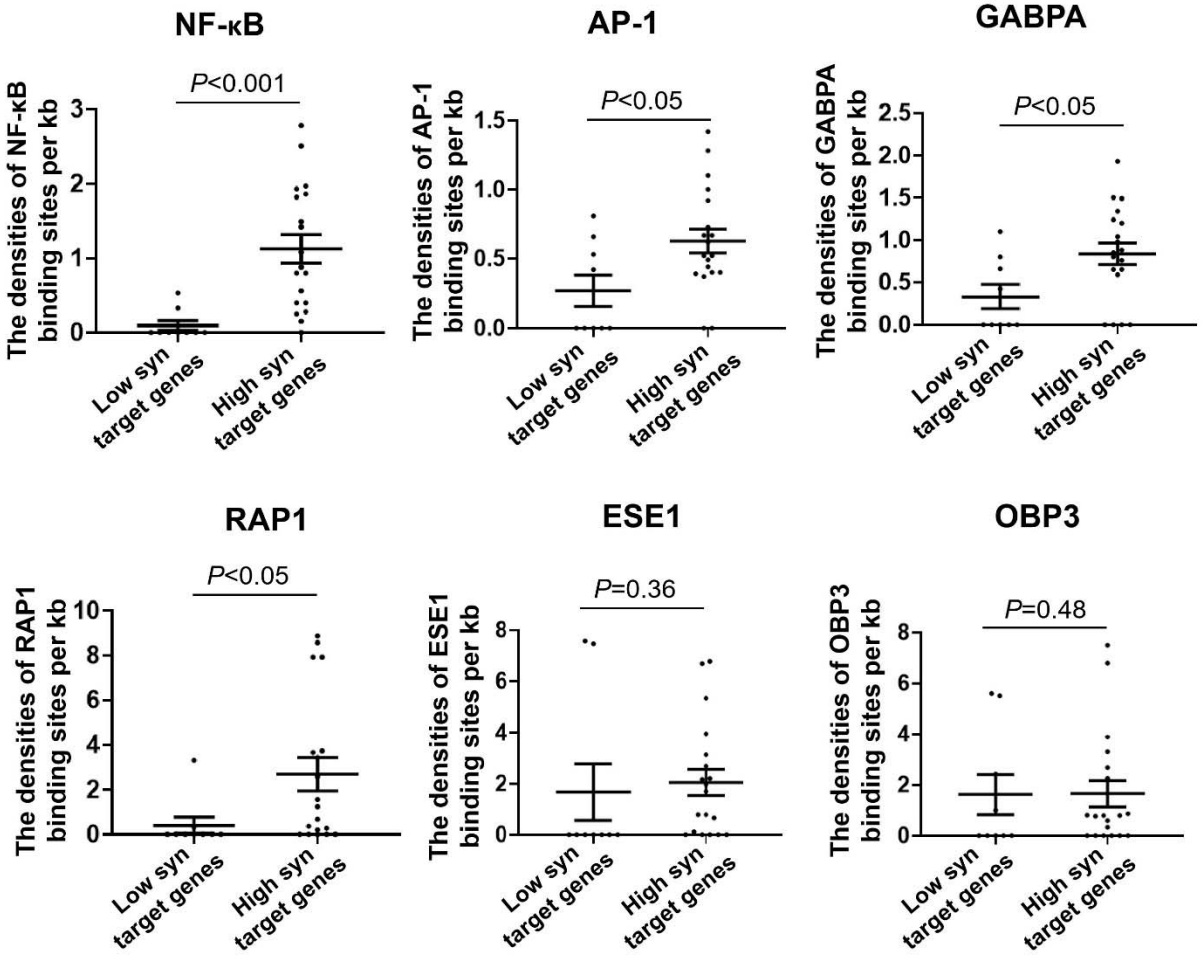
NF-κB
P<0.001
The densities of NF-κB binding sites per kb
AP-1
P<0.05
The densities of AP-1 binding sites per kb
GABPA
P<0.05
The densities of GABPA binding sites per kb
RAP1
P<0.05
The densities of RAP1 binding sites per kb
ESE1
P=0.36
The densities of ESE1 binding sites per kb
OBP3
P=0.48
The densities of OBP3 binding sites per kb
Low syn target genes
High syn target genes

295

Figure 5. The AP-1, NF-κB, GABPA, and RAP1 binding motifs are enriched in the regions with increased chromatin accessibility in the IL-33 and IgECL-upregulated genes. A. Transcription factor binding motifs enriched in the regions with increased chromatin accessibility. Data represent two biological samples. **B.** The numbers of AP-1, NF-κB, GABPA, RAP1, ESE1 and OBP3 binding motifs in the low and high synergy target genes. The densities of transcription factor binding sites in the increased narrow peaks were normalized by the sizes of narrow peaks and expressed as the number of binding sites per kilobase. Low synergy target genes (Low syn target genes); High synergy target genes (High syn target genes). *P* values were calculated using one-tailed Student's *t* test.

We analyzed transcription factor binding motifs in the chromatin accessible areas that were upregulated by the combined IgECL and IL-33 stimulation relative to IgECL or IL-33 alone using MEME ChIP. We found that NF-κB, AP-1, OBP3, ESE1/ERF5, DAF-12/RAP1, and GABPA/ELK4 binding motifs were significantly enriched in the increased narrow peaks (**Figure 5, *A***). Because the enrichment of transcription factor binding motifs was measured in all genes that responded to the combined IgECL and IL-33 stimulation, we determined whether the high synergy target genes would differ from the low synergy target genes in the numbers of transcription factor binding motifs. We counted the number of binding sites for the putative transcription in the increased narrow peaks of the low versus the high synergy target genes. We showed that the average numbers of NF-κB binding sites found in the chromatin accessibility areas of the high synergy target genes were 11.7-fold more than that in the low synergy target genes (**Figure 5, *B***). Similarly, AP-1 binding sites were found to be elevated in the high synergy target genes (2.3-fold increase). Interestingly, we found more GABPA binding sites, transcription factors capable of interacting with purine rich repeats (GA repeats) and a paralog gene of ETS2, in the regions with increased chromatin accessibility in the high synergy target genes. RAP1, an orthologous to human TERFIP, also showed 6.6-fold increase in binding sites in the high synergy target genes. In contrast, OBP3 and ESE1 binding sites did not increase in

the high synergy target genes relative to low synergy target genes (**Figure 5, *B***). Our results suggest that whether genes can respond to the combined IgECL and IL-33 stimulation are predetermined by the transcriptional codes embedded in the gene sequences and that the combined IgECL and IL-33 stimulation might achieve greater synergy in promoting gene transcription of the high synergy target genes by binding to denser NF-κB, AP-1, GABPA and RAP1 binding sites.

Discussion

Epithelial cell-derived cytokine IL-33 has been reported to promote inflammation-mediated by IgE and MCs, implicating how epithelial cell damage during infections can promote allergic inflammation during asthma attack and atopic dermatitis exacerbation. However, genes promoted by the combined IgECL and IL-33 stimulation have not been investigated genome-wide. While our findings that *CCL1*, *CCL2*, *CXCL1*, *CXCL2*, *CXCL8*, *IL1B*, *IL5*, *IL6*, *IL13* gene transcription were promoted the combined antigen and IL-33 stimulation were previously reported (Silver et al. 2010; Bawazeer and Theoharides 2019; Franke et al. 2021), the majority of genes were promoted by the combined antigen and IL-33 stimulation haven't been reported before. These newly found genes promoted by the combined IgECL and IL-33 stimulation encode signal molecules, transcription factors, cell survival and cell death, and receptor and receptor binding.

One of the key findings from our k means clustering analysis is that the combined antigen and IL-33 stimulation upregulated many genes encoding molecules involved in the NF-κB signaling pathway. Antigenic stimulation through IgE receptor cross-linking is a potent activator of transcription factors NFAT and NF-κB (Blank et al. 2021), and IL-33 is a potent activator of NF-κB (Martin and Martin 2016). Although IL-33 or IgECL stimulation alone is sufficient to promote transcription of NFKB1, REL, GBP2 and RIPK2, when combined, they elicit much stronger NFKB1, REL, GBP2 and RIPK2 gene transcription. Given that *NFKB1* (also known as p50) and *REL* (also known as p68) are the two subunits of NF-κB transcription factor complex and that GBP2, a guanine-binding protein, RIPK2, a member of the receptor-interacting protein (RIP) family of serine/threonine protein kinases, are known potent activator of the NF-κB

pathway, upregulated gene transcription can form positive feed-forward loops to strengthen NF-κB signaling, leading to synergistic transcriptional outputs of NF-κB target genes, including *IL1B*, *IL6*, *CXCL8*, *TNF*, *CCL2* (*MCP1*), *CXCL1* (Liu et al. 2017). A previous study used rat basophilic leukemia MCs, RBL-2H3 to demonstrate that multiple copies of NF-κB and NFAT binding sites were critical in antigen and IL-33 stimulation-driven reporter gene transcription. Our transcription factor motif analysis on chromatin accessible regions that were promoted by combined IL-33 and antigen stimulation indeed established significantly enriched NF-κB binding motif and AP-1 binding motif, supporting previous conclusion that IL-33 and antigenic stimulations synergistically activate NF-κB and NFAT to promote gene transcription of pro-inflammatory cytokines and chemokines *TNF*, *IL6*, *IL13*, *CCL2* (*MCP1*), *CCL7* (*MCP3*) and *CCL3* (*MIP1A*) (Andrade et al. 2011).

Interestingly, we also found potential negative feedback loops formed by TNFAIP2, TNFAIP3, NFKB1A, and NFKB1Z whose coding genes were significantly increased by the combined IL-33 and antigen stimulation. Therefore, upregulation of these gene transcriptions might provide critical control of NF-κB activation.

In addition to NF-κB binding motif and AP-1 binding motifs, we found more binding sites in the chromatin accessible regions that were promoted by combined IL-33 and antigen stimulation for GABPA, which binds to GA repeats and is a paralog gene of ETS2. While GABPA mRNA was expressed at low level revealed by our RNA-seq analysis, several ETS2 family transcription factor genes *ETS2*, *ELK1*, *ELF1*, *SPI1*, whose gene products can bind to GABPA binding site, were expressed in HSMCs. Whether these ETS2 family transcription factors can be recruited to

bind GABPA binding sites in response to the combined antigen and IL-33 stimulation remains to be determined. RAP1 is encoded by a gene named *TERF2IP* (Deregowska and Wnuk 2021). RAP1 interacts with transcription factor TERF2 to binds consensus sequences TTAGGG found next to AP1, NF-κB and GABPA binding sites (Arat and Griffith 2012). We found that TERF2 is expressed in HMSCs. TERF2 is known to involve in telomere maintenance and protection against end-to-end fusion of chromosomes. Knockdown of RAP1 reduced NF-κB activity and NF-κB -dependent pro-inflammatory cytokines in THP-1 macrophages (Cai et al. 2015). Because transfection of primary HSMCs is challenging, the precise functional role of ETS2 family transcription factors and RAP1 in mediating the IL-33 and IgECL synergy remains to be established and will be a subject for further investigation.

In summary, because IL-33 can be released by injured epithelial cells during infection, our findings that synergistically upregulation of pro-inflammatory cytokine and chemokine genes by the combination of antigen and IL-33 stimulations might provide some clues for future investigation into mechanisms underlying IL-33-caused exacerbation of allergic inflammation.

Materials and Methods

Human skin mast cell (HSMC) culture

De-identified fresh skin biopsies were obtained after breast reduction or mastectomy from the Cooperative Human Tissue Network of the National Cancer Institute. Handling human skin tissues was approved by the University of South Carolina Institutional Review Board. Human skin MCs were cultured from human skin essentially as described (Kambe et al. 2001; Caslin et al. 2018). After removing subcutaneous fat by blunt dissection, residual tissue was cut into 1- to 2-mm fragments then digested with type 2 collagenase (1.5 mg/ml), hyaluronidase (0.7 mg/ml), and type 1 DNase (0.15 mg/ml) in HBSS for 1 h at 37°C, for a total of three cycles of 1 h digestion. After each cycle, the dispersed cells were collected by filtering through a no. 80 mesh sieve and suspended in HBSS containing 1% FCS and 10 mM HEPES. Cells were suspended in HBSS, layered over a Percoll cushion, and centrifuged at 700 × *g* at room temperature for 20 min. Nucleated cells were collected from the buffer/Percoll interface. Cells enriched by Percoll density-dependent sedimentation were adjusted to a concentration of 1×10^6 cells/ml in serum-free X-VIVO™ 15 medium (Lonza BioWhittaker) containing 100 ng/ml recombinant human SCF (Peprotech) in 24-well plates. The culture medium was changed weekly, and wells were split when cell concentration doubled. The percentages of mast cells were assessed cytochemical by metachromatic staining with toluidine blue. Mature mast cells at ~ 100% purity and viability are obtained by 6-8 weeks of culture, and 8- to 16-week-old mast cells were used in these experiments. HSMCs were shipped to the Huang laboratory at National Jewish Health for RNA-seq and qPCR analysis.

HSMCs stimulations

IgE receptor cross-linking (IgECL) on HSMCs was accomplished through sensitization with 1 μg/mL chimeric human IgE anti-NP antibody (MCA333S, BIO-RAD, Hercules, CA) for 24 hours. The sensitized HSMCs were challenged with 100 ng/mL NP-HSA (N-5059, LGC, Petaluma, CA) for two additional hours. For single or combined cytokine and IgECL treatments, IL-33 (50 ng/mL, 200-33, PEPROTECH, Cranbury, NJ), TSLP (50 ng/mL, 300-62, PEPROTECH, Cranbury, NJ) or IL-25 (50 ng/mL, 200-24, PEPROTECH, Cranbury, NJ) were added to HSMCs for a total of 26 hours.

RNA-seq

Total RNA was extracted from HSMCs that were untreated or treated with various stimuli using the RNeasy mini kit (Qiagen, Valencia, CA) according to the manufacturer's protocol. The RNA-seq libraries were prepared as described before (Li et al. 2021). Briefly, the quality of input RNA was analyzed by running the RNA sample on the 4150 TapeStation System (Agilent, CA). PolyA mRNA was isolated using the NEBNext® Poly(A) mRNA magnetic isolation module (E7490, New England Biolabs, Ipswich, MA). RNA-seq libraries were obtained using the NEB-Next® Ultra™ II RNA library prep kit for Illumina® (E7770S, New England Biolabs, Ipswich, MA). The isolated mRNA was fragmented, reverse transcribed into cDNA, end-repaired, and adapter-ligated. The ligated samples were digested by USER enzyme, amplified by PCR, and purified using AMPure-XP beads (Beckman Coulter Life Sciences, A63881, Indianapolis, IN). The quantity and quality of RNA libraries were assessed on an Agilent Technologies 2100 Bioanalyzer. Paired-ended sequencing of the RNA libraries was performed on an Illumina NovaSEQ6000 platform.

Omni-ATAC-seq

Omni-ATAC-seq, an improved ATAC-seq protocol, was performed according to the published method (Corces et al. 2017; Li et al. 2021). Briefly, 50,000 HSMCs that were untreated, treated with IL-33 alone, or IgECL with or without IL-33 were spun down and washed once with cold PBS. The cells were resuspended in 50 μl cold ATAC-RSB-lysis buffer and incubated for 3 minutes. The ATAC-RSB-lysis buffer was immediately washed out with 1 mL ATAC-RSB buffer. The cell pellet was resuspended in 50 μl transposition mix and incubated for 30 minutes at 37 °C. The reaction was stopped by adding 2.5 μl pH 8 0.5 M EDTA. The Qiagen MiniElute PCR purification kit (Qiagen) was used to purify the transposed DNA. Purified DNA was amplified using the following condition: 72°C for 5 min, 98 °C for 30 s, and 13 cycles: 98 °C for 10s, 63 °C for 30 s, 72 °C for 1min. The amplified libraries were purified, size-selected, and the quality and quantity of libraries were assessed on 4150 TapeStation System (Agilent, CA). The pair-ended sequencing of DNA libraries was performed on an Illumina NovaSEQ6000 platform.

RNA-seq data analysis

The RNA-seq data was analyzed as described before (Li et al. 2021). Briefly, the raw reads (average 20 million paired-end reads, two biological replicates for each treatment) were analyzed and quality checked by FastQC. The reads were aligned to the hg38 reference genome using the Spliced Transcripts Alignment to a Reference (STAR, version 2.4.0.1) software. Reads (FPKM) were assembled into reference transcripts and counted using Cufflinks (version 2.2.1). The average reads from two biological samples were calculated using Cuffmerge (version 1.0.0). The differential gene expression between the resting and stimulated samples was analyzed using

Cuffdiff (version 2.2.1). K-means clustering was performed using pheatmap (version 1.0.12). The optimal numbers of K in the RNA-seq datasets were determined using R packages Tidyverse (version 1.3.1), Cluster (version 2.1.0), Factoextra (version 1.0.7), and GridExtra (2.3). Genes in clusters were extracted using pheatmap (version 1.0.12).

Omni-ATAC-seq data analysis

The Omni-ATAC-seq data was analyzed as described before (Li et al. 2021). Briefly, raw sequencing reads (average 80 million paired-end reads, two biological replicates for each treatment) were aligned to the hg38 reference genome using Bowtie2 with very-sensitive and -x 2000 parameters. The read alignments were filtered using SAMtools to remove mitochondrial genome and PCR duplicates. Broad peaks and narrow peaks were called by MACS2 with the q-value cut-off of 0.05, and the sequencing data was displayed using Integrative Genomics Viewer (IGV).

Quantitative RT-PCR

For mRNA expression analysis, the HSMCs were untreated, treated with IL-33 or IgECL alone or in combination. Total RNA from HSMCs was isolated with TRIzol™ Reagent according to the manufacturer's instructions. cDNA was synthesized by reverse transcription. Quantitative PCR was performed in a QuantStudio 7 Flex Real-Time PCR System (ThermoFisher, MA). The sequences of qPCR primers are listed in **Table E7**. Relative mRNA amounts were calculated as follows: Relative mRNA amount = $2^{[\mathrm{Ct}(\textit{Sample})-\mathrm{Ct}(\textit{HPRT})]}$.

DAVID GO analysis

Gene ontology enrichment analysis was performed on genes that responded to the synergistic stimulations of IgECL plus IL-33 by using the Database for Annotation, Visualization, and Integrated Discovery (DAVID, version 6.8). The top-ranked genes in each enriched category were selected for heatmap representations using an Excel spreadsheet.

Assigning regulatory regions to genes

Binding and Expression Target Analysis (BETA) minus (Version 1.0.7) used to calculate the regulatory potential score and assign the regulatory regions identified by Omi-ATAC-seq to their putative target genes (Wang et al. 2013) with the following setting: Reference genome, Human: GRCh38; Distance: within 100 kb upstream and 100 kb downstream from the transcriptional start site of the gene.

DiffBind

For analysis of activation-induced accessible regions, Omni-ATAC-seq reads of HSMCs samples that were treated with IL-33 and IgECL were compared with those of HSMCs samples treated with IL-33 or IgECL using the R package DiffBind (version 2.10.0). The sequences of the regions that showed activation-induced Omni-ATAC-seq reads were used for TF binding motif enrichment analysis using MEME-ChIP (Version 5.4.1). The number of upregulated peaks in the low and high synergy genes were calculated by adding the number of short peaks within 100 kb upstream and 100 kb downstream from TSS were significantly increased in response to the combined IL-33 and IgECL stimulation relative to IL-33 or IgECL.

TF binding motif enrichment analysis

Multiple Em for Motif Elicitation (MEME)-ChIP performs comprehensive motif analysis on large sets of sequences such as those identified by ChIP-seq or CLIP-seq experiments. MEME-ChIP was used to identify the TF binding motifs enriched in accessible regions. To identify the TF binding motifs enriched in the induced accessible regions, BED files of IgE-stimulated and IgE+IL-33-stimulated were uploaded to the Find Individual Motif Occurrences (FIMO) tool of MEME (FIMO). The number of transcription factor binding sites in the increased narrow peaks of the low and high synergy genes was calculated by adding the number of transcription factor binding sites within the narrow peaks. The densities of transcription factor binding sites in the increased narrow peaks were normalized by the sizes of narrow peaks and expressed as the number of binding sites per kilobase.

Statistical analysis

One-tail Fisher Exact probability value was used for GO analysis. One-tailed Student's *t*-test was used to determine significant differences between the two treatment groups. Identifying statistically significantly differentially bound sites in DiffBind used specifical statistical methods built in the Bioconductor packages EdgeR and DEseq2.

Data access

All raw and processed sequencing data generated in this study have been submitted to the NCBI Gene Expression Omnibus (GEO; https://www.ncbi.nlm.nih.gov/geo/) under accession number GSE196895. The RNA-seq data can be found in the GEO database: "GSE196862"; The ATAC-seq data can be found in the GEO database: "GSE196883".

Acknowledgments

We thank lab members for the thoughtful discussions. We are grateful to Dr. Bifeng Gao and the staff of the Genomics Shared Resource Facility at the University of Colorado Cancer Center for Next-Generation Sequencing.

Funding

Supported by grants from the National Institutes of Health R01AI107022 and R01AI135194 (H.H.), National Institutes of Health (NIH)/National Institute of General Medical Sciences (NIGMS) Pilot Project P20GM103641 (C.A.O. and G.G.), a fund provided by a fellowship from the Higher Committee for Education Development (HCED) and Ministry of Higher Education and Scientific Research (MOHSR) in Iraq (Z.M.).

Declaration of interests

The authors declare no competing interests.

References

Akula S, Paivandy A, Fu Z, Thorpe M, Pejler G, Hellman L. 2020. Quantitative In-Depth Analysis of the Mouse Mast Cell Transcriptome Reveals Organ-Specific Mast Cell Heterogeneity. *Cells* **9**.

Allakhverdi Z, Comeau MR, Jessup HK, Yoon BR, Brewer A, Chartier S, Paquette N, Ziegler SF, Sarfati M, Delespesse G. 2007a. Thymic stromal lymphopoietin is released by human epithelial cells in response to microbes, trauma, or inflammation and potently activates mast cells. *The Journal of experimental medicine* **204**: 253-258.

Allakhverdi Z, Smith DE, Comeau MR, Delespesse G. 2007b. Cutting edge: The ST2 ligand IL-33 potently activates and drives maturation of human mast cells. *J Immunol* **179**: 2051-2054.

Andrade MV, Iwaki S, Ropert C, Gazzinelli RT, Cunha-Melo JR, Beaven MA. 2011. Amplification of cytokine production through synergistic activation of NFAT and AP-1 following stimulation of mast cells with antigen and IL-33. *European journal of immunology* **41**: 760-772.

Araki T, Milbrandt J. 1996. Ninjurin, a novel adhesion molecule, is induced by nerve injury and promotes axonal growth. *Neuron* **17**: 353-361.

Arat NO, Griffith JD. 2012. Human Rap1 interacts directly with telomeric DNA and regulates TRF2 localization at the telomere. *The Journal of biological chemistry* **287**: 41583-41594.

Bawazeer MA, Theoharides TC. 2019. IL-33 stimulates human mast cell release of CCL5 and CCL2 via MAPK and NF-kappaB, inhibited by methoxyluteolin. *European journal of pharmacology* **865**: 172760.

Blank U, Huang H, Kawakami T. 2021. The high affinity IgE receptor: a signaling update. *Current opinion in immunology* **72**: 51-58.

Brown LF, Detmar M, Claffey K, Nagy JA, Feng D, Dvorak AM, Dvorak HF. 1997. Vascular permeability factor/vascular endothelial growth factor: a multifunctional angiogenic cytokine. *EXS* **79**: 233-269.

Burns JM, Summers BC, Wang Y, Melikian A, Berahovich R, Miao Z, Penfold ME, Sunshine MJ, Littman DR, Kuo CJ et al. 2006. A novel chemokine receptor for SDF-1 and I-TAC involved in cell survival, cell adhesion, and tumor development. *The Journal of experimental medicine* **203**: 2201-2213.

Cai Y, Sukhova GK, Wong HK, Xu A, Tergaonkar V, Vanhoutte PM, Tang EH. 2015. Rap1 induces cytokine production in pro-inflammatory macrophages through NFkappaB signaling and is highly expressed in human atherosclerotic lesions. *Cell Cycle* **14**: 3580-3592.

Caslin HL, Taruselli MT, Paranjape A, Kiwanuka K, Haque T, Chumanevich AP, Oskeritzian CA, Ryan JJ. 2018. The Use of Human and Mouse Mast Cell and Basophil Cultures to Assess Type 2 Inflammation. *Methods Mol Biol* **1799**: 81-92.

Chhiba KD, Hsu CL, Berdnikovs S, Bryce PJ. 2017. Transcriptional Heterogeneity of Mast Cells and Basophils upon Activation. *J Immunol* **198**: 4868-4878.

Cildir G, Toubia J, Yip KH, Zhou M, Pant H, Hissaria P, Zhang J, Hong W, Robinson N, Grimbaldeston MA et al. 2019. Genome-wide Analyses of Chromatin State in Human Mast Cells Reveal Molecular Drivers and Mediators of Allergic and Inflammatory Diseases. *Immunity* **51**: 949-965 e946.

579 Corces MR, Trevino AE, Hamilton EG, Greenside PG, Sinnott-Armstrong NA, Vesuna S, Satpathy
580 AT, Rubin AJ, Montine KS, Wu B et al. 2017. An improved ATAC-seq protocol reduces
581 background and enables interrogation of frozen tissues. *Nat Methods* **14**: 959-962.
582 Decker EL, Nehmann N, Kampen E, Eibel H, Zipfel PF, Skerka C. 2003. Early growth response
583 proteins (EGR) and nuclear factors of activated T cells (NFAT) form heterodimers and
584 regulate proinflammatory cytokine gene expression. *Nucleic Acids Res* **31**: 911-921.
585 Deregowska A, Wnuk M. 2021. RAP1/TERF2IP-A Multifunctional Player in Cancer Development.
586 *Cancers (Basel)* **13**.
587 Dvorak HF, Orenstein NS, Carvalho AC, Churchill WH, Dvorak AM, Galli SJ, Feder J, Bitzer AM,
588 Rypysc J, Giovinco P. 1979. Induction of a fibrin-gel investment: an early event in line 10
589 hepatocarcinoma growth mediated by tumor-secreted products. *J Immunol* **122**: 166-
590 174.
591 Franke K, Wang Z, Zuberbier T, Babina M. 2021. Cytokines Stimulated by IL-33 in Human Skin
592 Mast Cells: Involvement of NF-kappaB and p38 at Distinct Levels and Potent Co-
593 Operation with FcepsilonRI and MRGPRX2. *Int J Mol Sci* **22**.
594 Galli SJ, Grimbaldeston M, Tsai M. 2008. Immunomodulatory mast cells: negative, as well as
595 positive, regulators of immunity. *Nature reviews Immunology* **8**: 478-486.
596 Gurish MF, Austen KF. 2001. The diverse roles of mast cells. *The Journal of experimental*
597 *medicine* **194**: F1-5.
598 Han NR, Oh HA, Nam SY, Moon PD, Kim DW, Kim HM, Jeong HJ. 2014. TSLP induces mast cell
599 development and aggravates allergic reactions through the activation of MDM2 and
600 STAT6. *J Invest Dermatol* **134**: 2521-2530.
601 Hattermann K, Held-Feindt J, Lucius R, Muerkoster SS, Penfold ME, Schall TJ, Mentlein R. 2010.
602 The chemokine receptor CXCR7 is highly expressed in human glioma cells and mediates
603 antiapoptotic effects. *Cancer Res* **70**: 3299-3308.
604 Hungness ES, Luo GJ, Pritts TA, Sun X, Robb BW, Hershko D, Hasselgren PO. 2002. Transcription
605 factors C/EBP-beta and -delta regulate IL-6 production in IL-1beta-stimulated human
606 enterocytes. *Journal of cellular physiology* **192**: 64-70.
607 Johnson EN, Seasholtz TM, Waheed AA, Kreutz B, Suzuki N, Kozasa T, Jones TL, Brown JH, Druey
608 KM. 2003. RGS16 inhibits signalling through the G alpha 13-Rho axis. *Nature cell biology*
609 **5**: 1095-1103.
610 Kambe N, Kambe M, Kochan JP, Schwartz LB. 2001. Human skin-derived mast cells can
611 proliferate while retaining their characteristic functional and protease phenotypes.
612 *Blood* **97**: 2045-2052.
613 Kato Y, Morikawa T, Kato E, Yoshida K, Imoto Y, Sakashita M, Osawa Y, Takabayashi T, Kubo M,
614 Miura K et al. 2021. Involvement of Activation of Mast Cells via IgE Signaling and
615 Epithelial Cell-Derived Cytokines in the Pathogenesis of Pollen Food Allergy Syndrome in
616 a Murine Model. *J Immunol* **206**: 2791-2802.
617 Kehrl JH, Sinnarajah S. 2002. RGS2: a multifunctional regulator of G-protein signaling. *The*
618 *international journal of biochemistry & cell biology* **34**: 432-438.
619 Keir ME, Liang SC, Guleria I, Latchman YE, Qipo A, Albacker LA, Koulmanda M, Freeman GJ,
620 Sayegh MH, Sharpe AH. 2006. Tissue expression of PD-L1 mediates peripheral T cell
621 tolerance. *The Journal of experimental medicine* **203**: 883-895.

Kumagai T, Miki T, Kikuchi M, Fukuda T, Miyasaka N, Kamiyama R, Hirosawa S. 1999. The proto-oncogene Bc16 inhibits apoptotic cell death in differentiation-induced mouse myogenic cells. *Oncogene* **18**: 467-475.

Lee HJ, Ahn BJ, Shin MW, Jeong JW, Kim JH, Kim KW. 2009. Ninjurin1 mediates macrophage-induced programmed cell death during early ocular development. *Cell death and differentiation* **16**: 1395-1407.

Li Y, Gao J, Kamran M, Harmacek L, Danhorn T, Leach SM, O'Connor BP, Hagman JR, Huang H. 2021. GATA2 regulates mast cell identity and responsiveness to antigenic stimulation by promoting chromatin remodeling at super-enhancers. *Nat Commun* **12**: 494.

Liu T, Zhang L, Joo D, Sun SC. 2017. NF-kappaB signaling in inflammation. *Signal Transduct Target Ther* **2**.

Lohning M, Stroehmann A, Coyle AJ, Grogan JL, Lin S, Gutierrez-Ramos JC, Levinson D, Radbruch A, Kamradt T. 1998. T1/ST2 is preferentially expressed on murine Th2 cells, independent of interleukin 4, interleukin 5, and interleukin 10, and important for Th2 effector function. *Proceedings of the National Academy of Sciences of the United States of America* **95**: 6930-6935.

Martin NT, Martin MU. 2016. Interleukin 33 is a guardian of barriers and a local alarmin. *Nature immunology* **17**: 122-131.

Moritz DR, Rodewald HR, Gheyselinck J, Klemenz R. 1998. The IL-1 receptor-related T1 antigen is expressed on immature and mature mast cells and on fetal blood mast cell progenitors. *J Immunol* **161**: 4866-4874.

Motakis E, Guhl S, Ishizu Y, Itoh M, Kawaji H, de Hoon M, Lassmann T, Carninci P, Hayashizaki Y, Zuberbier T et al. 2014. Redefinition of the human mast cell transcriptome by deep-CAGE sequencing. *Blood* **123**: e58-67.

Niture S, Gyamfi MA, Lin M, Chimeh U, Dong X, Zheng W, Moore J, Kumar D. 2020. TNFAIP8 regulates autophagy, cell steatosis, and promotes hepatocellular carcinoma cell proliferation. *Cell Death Dis* **11**: 178.

Noguchi M, Nakamura Y, Russell SM, Ziegler SF, Tsang M, Cao X, Leonard WJ. 1993. Interleukin-2 receptor gamma chain: a functional component of the interleukin-7 receptor. *Science* **262**: 1877-1880.

Noman MZ, Desantis G, Janji B, Hasmim M, Karray S, Dessen P, Bronte V, Chouaib S. 2014. PD-L1 is a novel direct target of HIF-1alpha, and its blockade under hypoxia enhanced MDSC-mediated T cell activation. *The Journal of experimental medicine* **211**: 781-790.

Pandey A, Ozaki K, Baumann H, Levin SD, Puel A, Farr AG, Ziegler SF, Leonard WJ, Lodish HF. 2000. Cloning of a receptor subunit required for signaling by thymic stromal lymphopoietin. *Nature immunology* **1**: 59-64.

Park LS, Martin U, Garka K, Gliniak B, Di Santo JP, Muller W, Largaespada DA, Copeland NG, Jenkins NA, Farr AG et al. 2000. Cloning of the murine thymic stromal lymphopoietin (TSLP) receptor: Formation of a functional heteromeric complex requires interleukin 7 receptor. *The Journal of experimental medicine* **192**: 659-670.

Saenz SA, Taylor BC, Artis D. 2008. Welcome to the neighborhood: epithelial cell-derived cytokines license innate and adaptive immune responses at mucosal sites. *Immunol Rev* **226**: 172-190.

Saluja R, Khan M, Church MK, Maurer M. 2015. The role of IL-33 and mast cells in allergy and inflammation. *Clin Transl Allergy* **5**: 33.

Saluja R, Zoltowska A, Ketelaar ME, Nilsson G. 2016. IL-33 and Thymic Stromal Lymphopoietin in mast cell functions. *European journal of pharmacology* **778**: 68-76.

Schmitz J, Owyang A, Oldham E, Song Y, Murphy E, McClanahan TK, Zurawski G, Moshrefi M, Qin J, Li X et al. 2005. IL-33, an interleukin-1-like cytokine that signals via the IL-1 receptor-related protein ST2 and induces T helper type 2-associated cytokines. *Immunity* **23**: 479-490.

Silver MR, Margulis A, Wood N, Goldman SJ, Kasaian M, Chaudhary D. 2010. IL-33 synergizes with IgE-dependent and IgE-independent agents to promote mast cell and basophil activation. *Inflamm Res* **59**: 207-218.

Sjoberg LC, Nilsson AZ, Lei Y, Gregory JA, Adner M, Nilsson GP. 2017. Interleukin 33 exacerbates antigen driven airway hyperresponsiveness, inflammation and remodeling in a mouse model of asthma. *Sci Rep* **7**: 4219.

Spitz F, Furlong EE. 2012. Transcription factors: from enhancer binding to developmental control. *Nature reviews Genetics* **13**: 613-626.

Vogler M. 2012. BCL2A1: the underdog in the BCL2 family. *Cell death and differentiation* **19**: 67-74.

Wang S, Sun H, Ma J, Zang C, Wang C, Wang J, Tang Q, Meyer CA, Zhang Y, Liu XS. 2013. Target analysis by integration of transcriptome and ChIP-seq data with BETA. *Nat Protoc* **8**: 2502-2515.

Yagami A, Orihara K, Morita H, Futamura K, Hashimoto N, Matsumoto K, Saito H, Matsuda A. 2010. IL-33 mediates inflammatory responses in human lung tissue cells. *J Immunol* **185**: 5743-5750.